Four dimensional particle tracking for biological applications

H. I. C. Dalgarno[1], P. A. Dalgarno[1], A. Putoud[1], C. C. Diez[1], A. Baird[1], S. G. Aitken[1], D. P. Towers[2], C. E. Towers[2], N.C. Angarita-Jaimes[2], S. Chen[2], D.J. Smith[3], J. C. Kirkman-Brown[3], J. Graham[4], R. J. Warburton[1] and A. H. Greenaway[1]

[1]School of Engineering and Physical Sciences, IIS (part of the Edinburgh Research Partnership), David Brewster Building, Riccarton, Edinburgh, EH14 4AS
[2] School of Mechanical Engineering, University of Leeds, Leeds, LS2 9JT
[3]Centre for Human Reproductive Science, Birmingham Woman's NHS Foundation Trust, Edgbaston Birmingham, UK, B15 2TT
[4]Cairn Research Limited, Graveney Road, Faversham , Kent , ME13 8UP

We acknowledge support from STFC

Email: H.I.C.Dalgarno@hw.ac.uk | Web: http://waf.eps.hw.ac.uk

Four Dimensional Imaging

The Experimental System

The Principle - A weak off-axis Fresnel lens, combined with a positive lens, delivers in-focus images of multiple object planes onto a single image plane (see Fig 1.).

How? – Quadratic curvature of the grating rulings applies a defocus phase term to any incident wavefront, the grating behaves as a lens with a different focal length in each diffraction order.

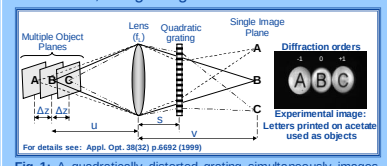

Fig 1: A quadratically distorted grating simultaneously images multiple object planes onto a single image plane

The grating properties determine the object plane separation (Δz), the image separation on the camera and the energy balance of the orders. Between 2 and 9 different planes can by imaged with approx. 82% optical efficiency.

For telecentric imaging the grating must be f_L from the lens, Opt. Exp. **14**(18) p.8269 (2006).

The Experiment – Nano-holes simulate fluorescent particles and a 100x microscope images them at Plane "B" (Fig.1). The grating-lens system produces multi-plane imaging about this plane. Precision nano-positioners translate the sample in 3D to provide experimental verification of our particle tracking algorithm.

Analysis : Depth Positioning using Image Sharpness

The Principle – Image Sharpness is a measure of image quality, that is dependent on the level of aberration present in the image. It can be used as an accurate metric for determination of range from a set of defocused images.

The grating-lens system (Fig.1) can image the same particle on 2 to 9 planes simultaneously. The particle's position in relation to the imaged planes determines the amount of defocus in each image of that particle. The calculated Image Sharpness of these images can be used to obtain an unambiguous measurement of its position in z.

How is it calculated? – Image Sharpness is the integrated area under the squared Modulation Transfer Function (MTF²) of a given image. It can also be calculated by integrating the square of the original intensity image.

Fig. 2 shows the area under the MTF decreasing as defocus aberration increases (i.e. Image Sharpness also decreases). Fig. 3 shows experimental sharpness data from a nano-hole tracked on 3 planes with the grating.

This technique could be easily applied to track multiple objects in real-time on a CMOS detector.

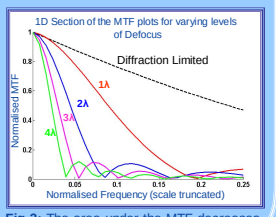

Fig 2: The area under the MTF decreases as wave-front aberration increases

Nano-Scale Particle Tracking with Image Sharpness

The Principle – An advantage of the grating method is it can provide multiple images of the same particle in each snapshot. The shape of a single sharpness curve means a single measured sharpness value could correspond to more than one z position. By comparing the sharpness values of the particle's image from more than one diffraction order this ambiguity is resolved.

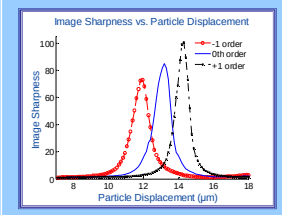

Fig 3: Image Sharpness vs. Particle Displacement - Experimental data tracking a single nanohole on 3 planes with the grating.

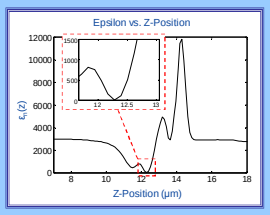

Fig 4: The error metric ε_n as a function of z for a single CCD snapshot image (where ε = 0 this is the unambiguous depth position of the particle)

Unambiguous z-Position Determination using a Least-Squares type approach:

A set of calibration data is taken using a single nano-hole, translated over a known depth range. The Image Sharpness for each diffraction order image in each snapshot is calculated and an example of this is shown in Fig 3.

The Problem - If we have a snapshot image "n", can we determine at which Z position this was captured?

The Solution - We compare the three sharpness values contained within this snapshot to all the other sharpness values in the calibration data using a Least-Squares like approach (see opposite). The error metric this produces will reach a global minimum when the best match to the three values is found. This is the unambiguous Z position.

The Future – We are now developing a Maximum Likelihood Estimation method, which so far looks to be very promising…

How to calculate the error metric:

$$\varepsilon_n(z) = \left(S_{-1}(n) - S_{-1}(z)\right)^2 + \left(S_0(n) - S_0(z)\right)^2 + \left(S_{+1}(n) - S_{+1}(z)\right)^2$$

$\varepsilon_n(z)$ = The error metric as a function of z for a given snapshot "n"
$S_{-1}(n)$ = Calculated sharpness value for the -1 order, in a given snapshot "n"
$S_{-1}(z)$ = The entire sharpness curve for the -1 order
$S_0(n)$ = As $S_{-1}(n)$ but this time for the 0th order.....etc

4D Imaging with Commercial Microscope Systems

We have now created a modular version of the equipment in Fig 1 designed to be a robust, light-tight, "bolt-on" 4D imaging system compatible with the CCD output port of any commercial microscope system (see Fig 5).

Collaboration – We work in close collaboration with several cell biology groups to apply 4D imaging to their different areas of research. So far, copies of this bolt-on system have been distributed to groups at Oxford and Manchester Universities. Copies of this system will be given to Bristol University and Birmingham Women's Hospital in the near future.

Versatility – The 4D bolt-on module is compatible with any microscope imaging mode. We have used this system successfully to capture 4D data in Bright Field, Dark Field, Fluorescence, Phase Contrast and DIC imaging modes. The system is fully compatible with both inverted and upright microscopes and has been implemented on both. The system's versatile, compact, and rugged design has been developed through interactions with our collaborators to make it a useful general purpose instrument.

The Future - We are now working on the next generation system which will deliver Broadband 4D imaging. We are looking forward to further collaboration with our current partners and investigation of more applications for this technique in Molecular and Systems Biology.

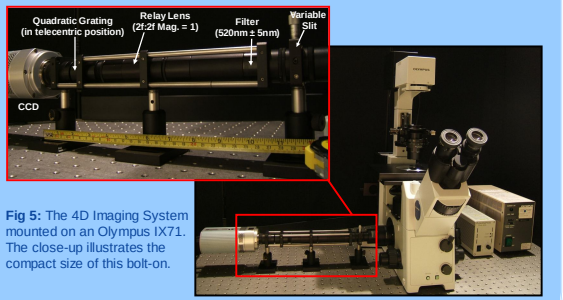

Fig 5: The 4D Imaging System mounted on an Olympus IX71. The close-up illustrates the compact size of this bolt-on.

Application Highlight: Sperm Motility Studies

The Research Interest – In human sperm motility studies the complex movement of the tail of the sperm cell is key to understanding how strongly the sperm is swimming.

The Current Technique – The overall length of the sperm tail, imaged in 2D, is used as a proxy to estimate the 3D configuration of the tail.

Advantage of our Technique – By imaging the sperm cells on multiple planes simultaneously we will be able to get a much clearer and more accurate 3D model of the tail's motion as it swims. By doing this in real-time we can, for example, study changes in the sperms motion as it approaches an egg.

Initial Tests – The data contained in Fig 6 are stills from real-time movies of human sperm swimming in viscous media. These were captured during a demonstration of the equipment at Birmingham Women's Hospital and show that imaging on both 3 and 9 planes would be viable for this application. While the gratings used here were not optimum for this example the results are promising and a version of the bolt-on 4Dimaging system will be given to Birmingham in the near future to explore this exciting application further.

Fig 6a:

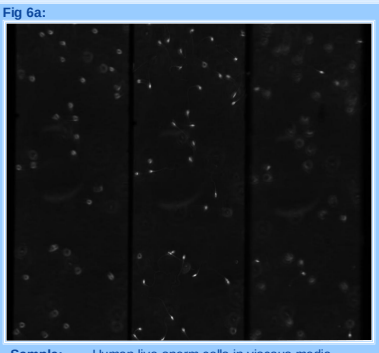

Sample: Human live sperm cells in viscous media
Illumination: Phase contrast imaging in white light (later filtered by the narrowband 3D optics to 520nm ±5nm)
3-D Imaging: Δz = 14.6μm

Fig 6b:

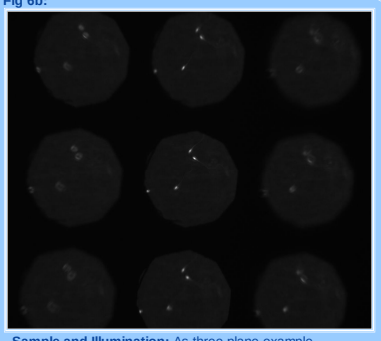

Sample and Illumination: As three plane example.
3-D Imaging: Nine plane imaging with "crossed" QD gratings (one with Δz = 3.66μm and one with Δz = 910nm)

Note: The grating period was not optimal for this CCD chip, resulting in overfilling in the vertical axis. Usually we design the gratings for use with a particular chip size to capture the largest field of view possible in each order.